As originally published in the IPC APEX EXPO Proceedings.

Analysis of the Design Variables of Thermoforming Process on the Performance of Printed Electronic Traces

Gill M., Gruner A.*, Ghalib N., Sussman M., Avuthu S., Wable G, Richstein J.
Jabil
St Petersburg, Florida, *Vienna, Austria

Abstract
One specific market space of interest to emerging printed electronics is In Mold Label (IML) technology. IML is used in many consumer products and white good applications. When combined with electronics, the In Mold Electronics (IME) adds compelling new product functionality. Many of these products have multi-dimensional features and therefore require thermoforming processes in order to prepare the labels before they are in-molded. While thermoforming is not a novel technique for IML, the addition of printed electronic functional traces is not well documented. There is little or no published work on printed circuit performance and design interactions in the thermoforming process that could inform improved IME product designs. A general full factorial Design of Experiments (DOE) was used to analyze the electrical performance of the conductive silver ink trace/polycarbonate substrate system. Variables of interest include trace width, height of draw, and radii of both top and bottom curvatures in the draw area. Thermoforming tooling inserts were fabricated for eight treatment combinations of these variables. Each sample has one control and two formed strips. Electrical measurements were taken of the printed traces on the polymer sheets pre- and post- forming with a custom fixture to evaluate the effect on resistance. The design parameters found to be significant were draw height and bottom radius, with increased draw and smaller bottom curvature radii both contributing to the circuits' resistance degradation. Over the ranges evaluated, the top curvature radii had no effect on circuit resistance. Interactions were present, demonstrating that circuit and thermoforming design parameters need to be studied as a system. While significant insight impacting product development was captured further work will be executed to evaluate different ink and substrate material sets, process variables, and their role in IME.

Introduction
Printed electronic technology is an additive printing process that creates an electronic circuit by depositing one or several layers of conductive ink onto a substrate. Substrate choices include conformable and stretchable plastic films. Additional functional inks may be printed on the circuits for passive and active components like resistors, insulators, and for protection of the circuit in end-use applications. The printed circuitry is application-dependent and may vary from simple passive to complex multi-layer structures. In-mold printed electronics is an emerging technology extending the integration possibilities of electronics into applications that have historically not been possible with traditional printed circuit board technology.

Thermoforming is a process utilizing heat and either vacuum or high gas pressure to form a softened thermoplastic film onto a mandrel of desired shape and size (*Figure 1*) [1]. The film is placed on the tooling plate, transported into the chamber that is then heated. The vacuum or gas pressure pushes the softened film down onto the tooling insert to take the shape. Though it is a widely used technology in forming thermoplastics for packaging, white goods, and consumer products, the integration of printed electronics into the thermoforming process is relatively recent. The impact of the thermoforming process on the perform circuitry and the respective product and process design guidelines are not fully un

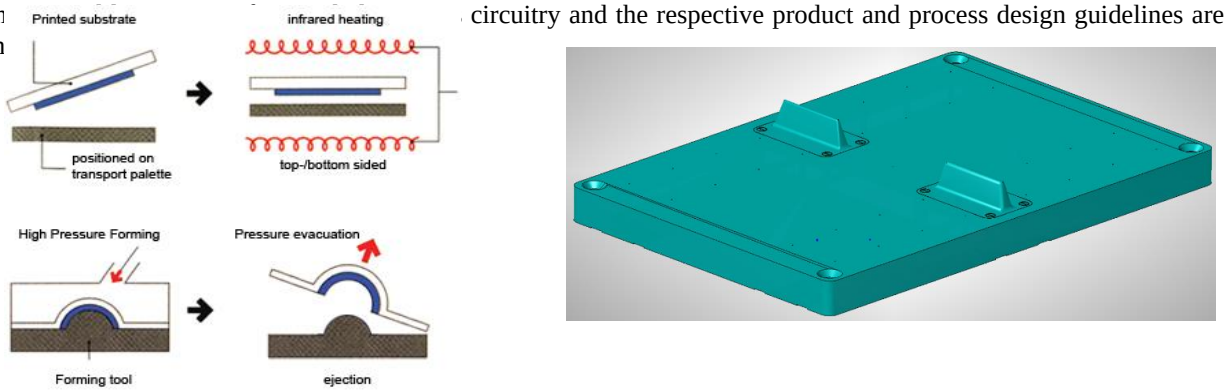

Figure 1 Schematic of a thermoforming process (left) and tooling plate (right)

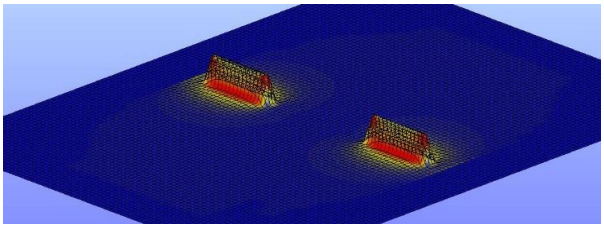

Figure 2 Simulation of the thermoformed test vehicle

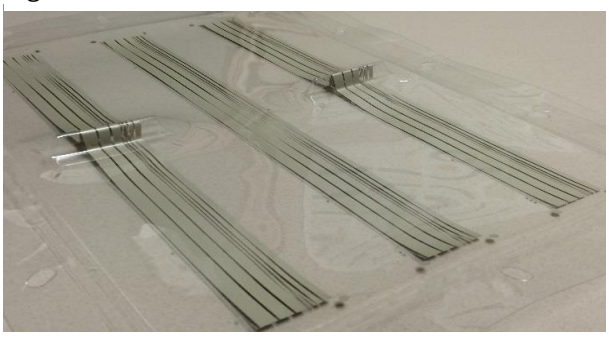

Figure 3 Thermoformed test vehicle

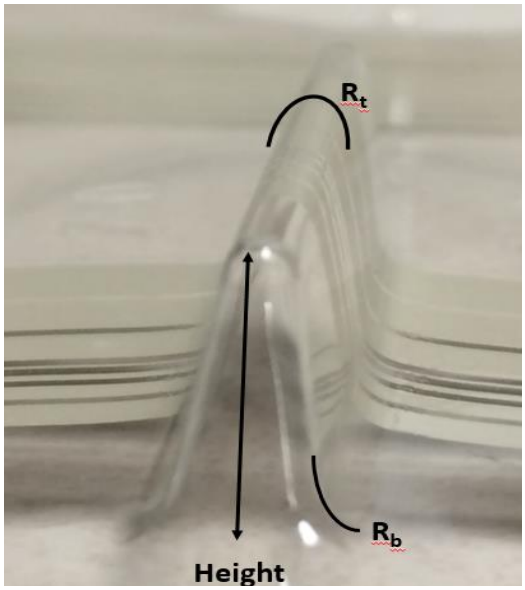

Figure 4 Design parameters studied on the test vehicle

The forming process moves substrate material and creates high stress areas within the substrate as it is forced to conform to the mandrel, potentially having adverse effects on printed trace performance and mechanical integrity (*Figure 2*). As the substrate and ink deforms conductive particles separate and compress impacting the conductivity. This change may be significant in some areas where discontinuity may lead to partial connectivity or catastrophic failure. This study focuses on three of the most likely mandrel design parameters that might adversely affect circuit performance: depth of draw (height), top radius (R_t), and bottom radius (R_b) (*Figure 3 & 4*). The experimental design was completed by evaluating the effect on printed electronic traces of five different widths over replaceable mandrel inserts in a thermoforming tool.

The results of these studies will provide the product designer with initial guidelines on how to compensate for anticipated electric conductivity degradation from thermoforming, minimizing costly prototyping and design iterations. Conceptually, the designer will eventually have access to a complete matrix of all needed information for electronic circuit design, suitable material sets, electronic trace geometry/conductivity relationships, and mechanical properties, within acceptable thermoforming limits.

Evaluating these thermoformed traces raises some interesting challenges and opportunities as there are major differences between thermoformed printed electronic traces and traditional Cu based PCBA electronic traces. There are a few assumptions that have to be made when evaluating these samples. When a product is thermoformed, the material does not have equal amount of draw and strain induced along the entire length of a trace. Inspections to investigate changes along the cross-sectional area are challenging to calculate along the entire trace. It is very difficult to measure the dimensional changes of the printed traces in all three dimensions, assuming no other performance impacting factors such as pin holes of polymer or varying conductive particle distribution in a printed trace. Particles need to be in contact together for current to flow, but this is not a bulk copper wire, where it is acceptable to assume a solid cross sectional area. In printed electronics, it is known that the "solids" part of the trace is actually more porous with a nonconductive polymer binding making up part of the trace (*Figure 5*) [2]. Other contributing factors not investigated here are the polymer structure from raw material processing, different molecular structures of ink and substrate processing methods varying from supplier to supplier, and differing elastic properties of the materials. For example, within a material, an amorphous versus crystalline structure may create areas with different internal stresses that can affect how the material is drawn during thermoforming. Different functional inks have different solids loading, particle shapes, and particle sizes, with varying distributions. This may be impacted by the homogeneity of the ink system due to mixing. These could have implications on how well the ink can conduct electrically before and after forming.

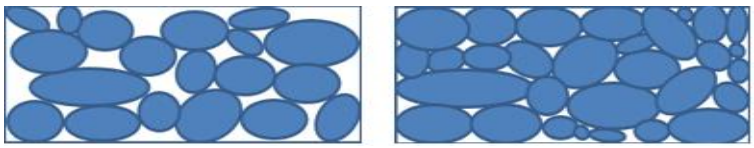

Figure 5 Conductive particles of different shapes and sizes distributed in a printed trace. Left image shows high porosity, less surface contact between particles resulting in a higher resistance trace. Right image shows a higher packing density trace closer to traditional solid PCB trace with lower resistance

Discussion of Methodology

The test vehicle contained three strips of eight parallel electronic traces per sample. Each trace had a different width, ranging from 5700 µm down to 150 µm *(Figure 6)*. The basic relationship of electric resistance as function of trace width should be an inverse parabolic curve. Since resistance is an inverse proportion to area, but the lengths are the same, those values cannot be compared directly in our test vehicle. A goal was to establish a lower trace width limit for which the trace could reliably be printed with the selected material set and screen. Consistent quality of formed prints was obtained down to 1700 µm, yielding five trace widths for inclusion in the experiment. The replaceable mandrel portion of the DOE was a full factorial, including three variables at two levels of the height, R_t, and R_b (*Table 1*). Eight different inserts were required to complete the study. With the inclusion of the five trace widths, the general full factorial experiment consisted of 40 trials. All printing, drying and forming parameters were held constant. A custom substrate test fixture with tooling holes allowed probing the traces in a consistent location (*Figure 7*). A programmable 6.5 digit multi-meter was used to collect trace resistance data. Each trace from all of the samples was measured three separate times, resulting in 600 data points.

Understanding the impact of key thermoforming process variables on electrical properties can help designers to select an appropriate trace width for a given geometric shape of a (to be) formed product. How the forming process affects the trace's cross-sectional area, particle distribution, packing density, and the mechanical integrity of the trace, will directly impact the electrical performance, and may gate product design. With forms and designs of thermoformed products that are more complex, multiple trace segments will change electrical performance of the electrical circuit.

Table 1 Design of experiments (DOE) factors, number of levels, and parameters

Factor	Number of Levels	Level Parameters
Trace width	5	X, X+1, X+2, X+3, X+4
Height	2	H, H+1
Top Radius	2	T, T+1
Bottom Radius	2	B, B+1

Figure 6 Test vehicle screen (left) and printed (right)

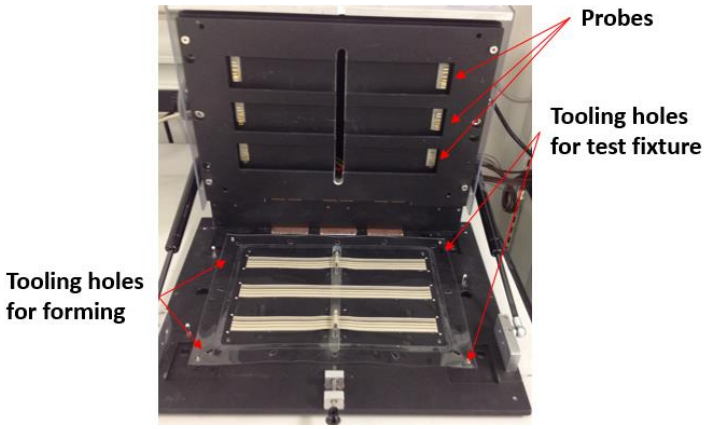

Figure 7 Custom electrical test fixture for resistance measurements

Results

Resistance measurements were taken pre and post forming to assess resistance changes introduced by the thermoforming process. The significant DOE factors were height, bottom radius and trace width, while the top radius was found not to be significant. The R_{sq} for the model of the analysis was 96.76 percent, adjusted R_{sq} is 96.58 percent, and predicted R_{sq} is 96.36 percent *Table 2* in Appendix. Residual plots are also included for reference in Appendix (*Figure 14*).

The factorial plot depicts the significance of height, bottom radius, and trace width on the formed electrical traces (*Figure 8)*. The top radius as a main factor had no impact. The shape of the curve for trace width is of parabolic type.

Normalizing resistance on the assumption the traces have constant resistivity and length and A (area) is w*h

- (w = width, h = height)
- $R = \rho\frac{L}{A} \propto \frac{1}{w*h}$; solving for h using the means of the plots: $h \propto \frac{1}{w*R} \approx 0.02$ average height parameter for all traces.
- The value of *h* is not assumed equivalent to the physical observable height-- it shows a consistent ink deposition.

An Analysis of Variance (ANOVA) was conducted separately per each trace width to ensure all trends for each trace were the same as the overall model. The mean trace resistance with increased forming height was 2.5 Ω, the top forming radius had a negligible impact, and bottom forming radius had a strong impact by decreasing mean trace resistance by 1.5Ω (*Figure 9*).

The slope differences in the plots indicate design interactions between height and bottom radius, height and trace width, and top radius and bottom radius (*Figure 10 & 11*). The factors that did not interact are top radius - trace width and top radius – height.

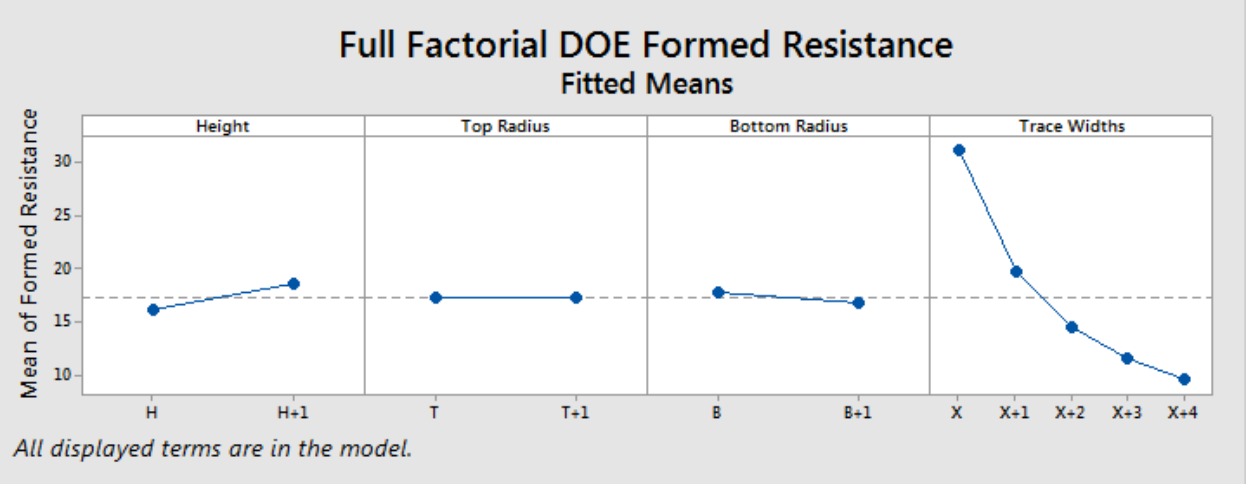

Figure 8 DOE factorial plot of post-formed mean resistance (Ω) for the full design

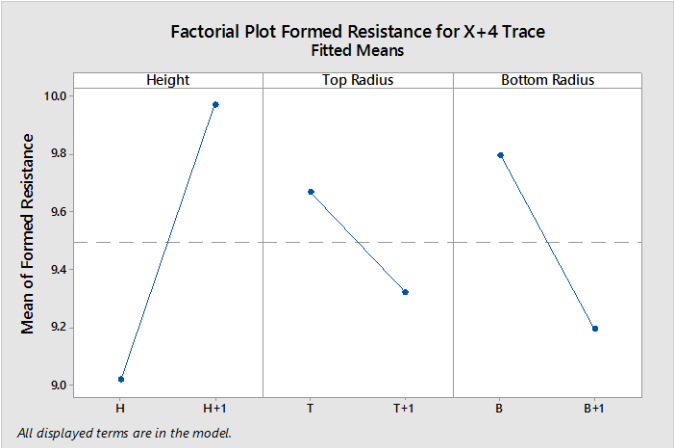

Figure 9 DOE factorial plot of post-formed mean resistance (Ω) for X+4 mm trace width

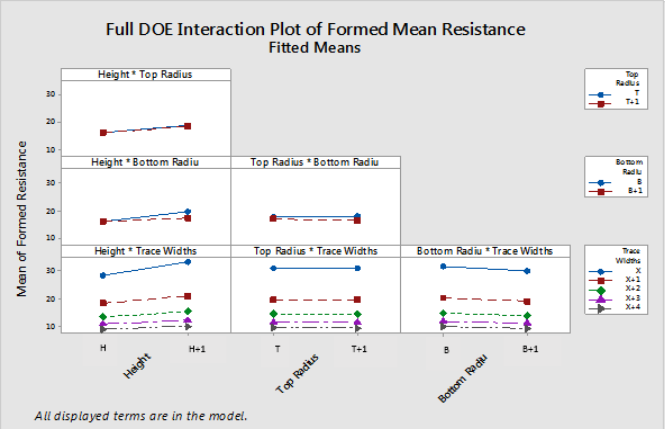

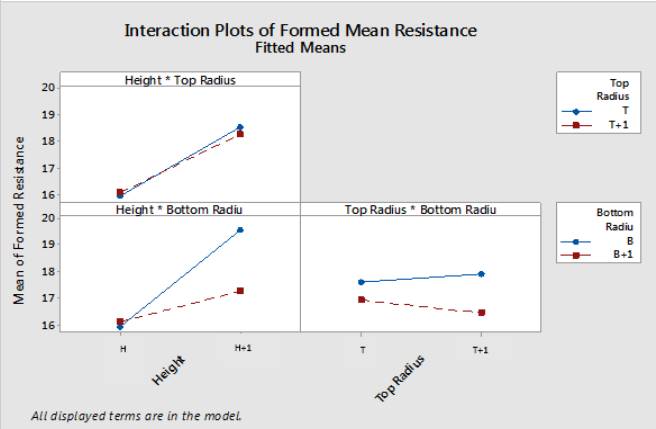

Figure 10 & 11 Interaction Plots for post-formed mean resistance (Ω) (left) full factorial DOE (right) for X+4 mm

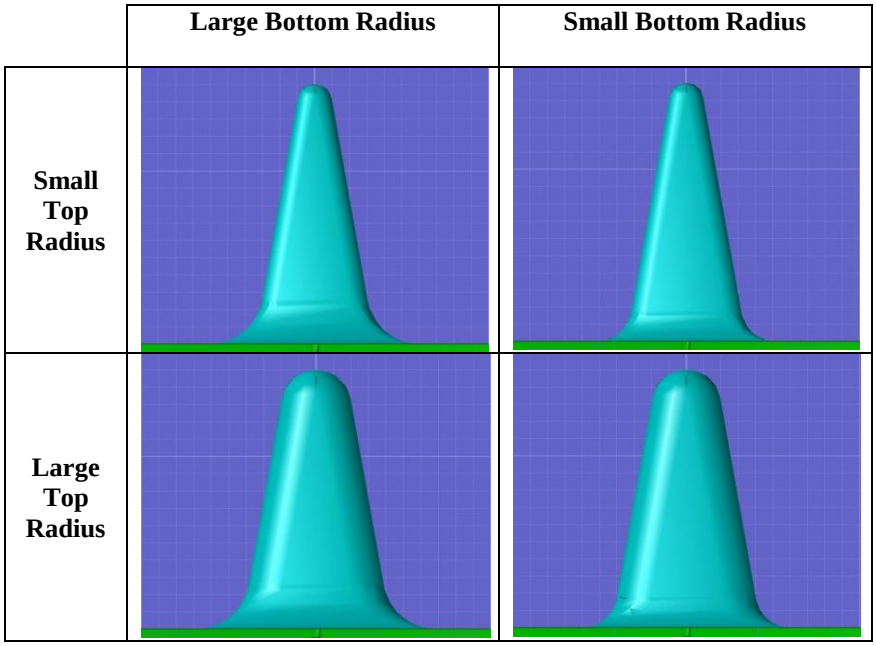

Figure 12 Quadrant figure of four varying cross-sectional sketch of the thermoformed parts

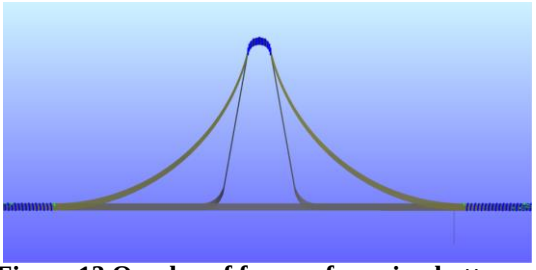

Figure 13 Overlay of forms of varying bottom radius, the bigger bottom radius undergoes less elongation

Discussion

In thermoforming, the stress concentrators within the draw region vary depending on some of these dominant geometric variables (*Figure 12*). The larger top radii limit material movement that can be shared along the flank of the draw during the forming process, resulting in a thinner wall thickness. Paired with a smaller bottom radius, which requires a deeper draw length the material is thinned further (*Figure 13*). This may increase trace cracking potential leading to a reduced or even catastrophic failure in electrical performance. The larger the required draw height required to meet the design of a product, the more susceptible the traces will become to these described failure. Electrical conductivity of the printed trace is subject to

counteracting mechanisms. The net effect will determine electrical conductivity. The negative effect of elongation due to particle separation can be offset by compression due to pressure and heat that increases contact between particles.

Conclusions

As expected, there is a parabolic mean variation of resistance as a function of trace width. This study did not consider variability and shape of the ink deposit, which could introduce other variance.

The wider the traces, the less the draw height impacts the electrical performance.

The sharper the bottom radius, the more stress is induced with an increased probability of trace discontinuities.

The top radius did not have an impact on the resistance changes after forming in the range studied as a main factor.

There were numerous design interactions between the design variables. At the lower draw height, the radius did not have an effect. However, as the draw height increased, it caused a large difference in resistance. This translates into product design and electrical operating limits.

This study covered a limited range of varying radii, however, additional levels in these factors will be included in later studies. Future investigations will address interactions in more detail to determine potential design trade-offs for product design and functionality.

Summary

This experiment provides insight into future design guidelines and process intellectual property (IP) for manufacturing printed electronic products. The design was a 40 trial experiment, investigating the effects of various design variables draw heights, curvatures, and printed trace widths. The observations and data of this full factorial DOE suggest there are multiple interactions of parameters. The main interaction appears to be the bottom curvature radius and the amount of draw that impact the electrical performance. Height and trace width, height and top radius also contribute significant p-values according to the ANOVA table. Complimentary work analyzing grid patterns deformation is being done. Future work will include different design windows and explore additional material sets in greater depth.

Acknowledgments

A special thank you to Doug Greenfield for his mentorship and guidance throughout the analysis of the research.

We would like to thank other noteworthy contributors, George Oxx and Gina Clifford, for their valuable time and efforts providing feedback.

We thank our appreciated intern Nicholas Conde for his assistance collecting hundreds of data points for the analysis.

Reference

[1] Niebling Form Technologie. C12.06.2009. Federal Republic of Germany: Niebling Form Technologie; [accessed 2016 Jun 6]. http://www.niebling-form.com/en/high-pressure-thermoforming/

[2] Banfield, D. 2000. Understanding and Measuring Electrical Resistivity in Conductive Ink and Adhesives. SGIA Journal (June 2000 Edition). [Accessed 2016 Sep 27]. http://www.conductivecompounds.com/pdf/sgia.pdf

Appendix

Table 2 ANOVA Table

Source	DF	Adj SS	Adj MS	F-Value	P-Value
Model	35	42232.8	1206.65	557.42	0.000
Linear	7	40987.1	5855.30	2704.88	0.000
Height	1	953.9	953.90	440.66	0.000
Top Radius	1	1.1	1.10	0.51	0.477
Bottom Radius	1	189.5	189.51	87.55	0.000
Trace Widths	4	39741.3	9935.32	4589.67	0.000
2-Way Interactions	15	691.2	46.08	21.29	0.000
Height*Top Radius	1	6.7	6.66	3.08	0.080
Height*Bottom Radius	1	255.6	255.56	118.06	0.000
Height*Trace Widths	4	343.3	85.82	39.64	0.000
Top Radius*Bottom Radius	1	26.1	26.10	12.06	0.001
Top Radius*Trace Widths	4	2.7	0.67	0.31	0.871
Bottom Radius*Trace Widths	4	33.1	8.28	3.82	0.004
3-Way Interactions	13	75.8	5.83	2.69	0.001
Height*Top Radius*Bottom Radius	1	8.1	8.07	3.73	0.054
Height*Top Radius*Trace Widths	4	30.7	7.66	3.54	0.007
Height*Bottom Radius*Trace Widths	4	23.4	5.85	2.70	0.030
Top Radius*Bottom Radius*Trace Widths	4	9.7	2.44	1.13	0.343
Error	654	1415.7	2.16		
Lack-of-Fit	4	4.3	1.09	0.50	0.736
Pure Error	650	1411.4	2.17		
Total	689	43648.5			

Model Summary

S	R-sq	R-sq(adj)	R-sq(pred)
1.47130	96.76%	96.58%	96.36%

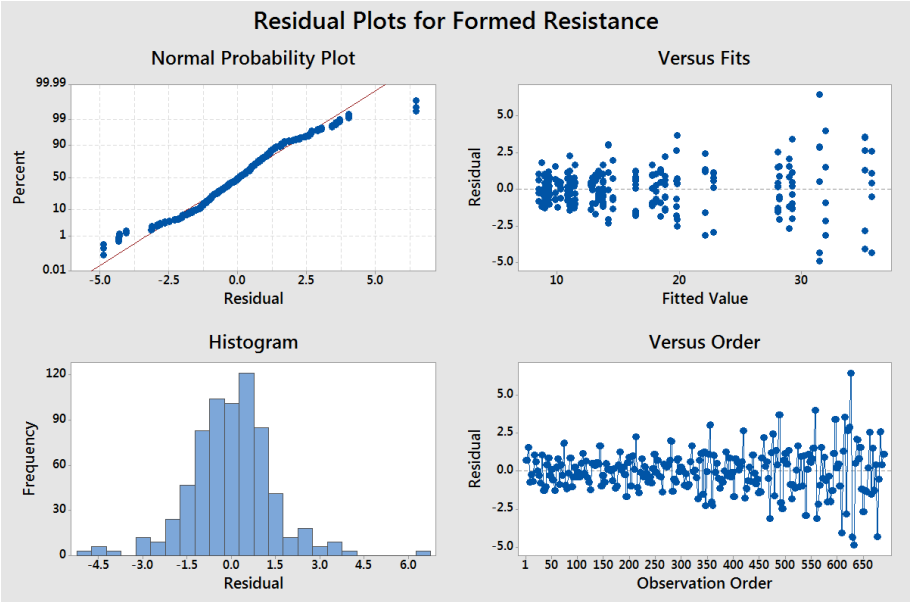

Figure 14 Residual plots for the full factorial DOE